



Original Article

Adipose Cells Induce Escape from an Engineered Human Breast Microtumor Independently of their Obesity Status

YOSEPH W. DANCE,¹ MACKENZIE C. OBERREDER,¹ ALEX J. SEIBEL,¹ TOVA MESHULAM,^{2,3}
JOSHUA W. OGONY,⁴ NIKHIL LAHIRI,¹ LAURA PACHECO-SPANN,⁵ DEREK C. RADISKY,⁴ MATTHEW D. LAYNE,³
STEPHEN R. FARMER,^{2,3} CELESTE M. NELSON,^{6,7} and JOE TIEN^{1,8}

¹Department of Biomedical Engineering, Boston University, 44 Cummington Mall, Boston, MA 02215, USA; ²Boston Nutrition Obesity Research Center, Boston University School of Medicine, Boston, MA, USA; ³Department of Biochemistry, Boston University School of Medicine, Boston, MA, USA; ⁴Department of Cancer Biology, Mayo Clinic Comprehensive Cancer Center, Jacksonville, FL, USA; ⁵Department of Quantitative Health Sciences, Mayo Clinic Comprehensive Cancer Center, Jacksonville, FL, USA; ⁶Department of Chemical and Biological Engineering, Princeton University, 303 Hoyt Laboratory, 25 William Street, Princeton, NJ 08544, USA; ⁷Department of Molecular Biology, Princeton University, Princeton, NJ, USA; and ⁸Division of Materials Science and Engineering, Boston University, Boston, MA, USA

(Received 30 August 2022; accepted 5 November 2022; published online 9 December 2022)

Associate Editor Michael R. King oversaw the review of this article.

Abstract

Introduction—Obesity is associated with increased breast cancer incidence, recurrence, and mortality. Adipocytes and adipose-derived stem cells (ASCs), two resident cell types in adipose tissue, accelerate the early stages of breast cancer progression. It remains unclear whether obesity plays a role in the subsequent escape of malignant breast cancer cells into the local circulation.

Methods—We engineered models of human breast tumors with adipose stroma that exhibited different obesity-specific alterations. We used these models to assess the invasion and escape of breast cancer cells into an empty, blind-ended cavity (as a mimic of a lymphatic vessel) for up to sixteen days.

Results—Lean and obese donor-derived adipose stroma hastened escape to similar extents. Moreover, a hypertrophic adipose stroma did not affect the rate of adipose-induced escape. When admixed directly into the model tumors, lean and obese donor-derived ASCs hastened escape similarly.

Conclusions—This study demonstrates that the presence of adipose cells, independently of the obesity status of the adipose tissue donor, hastens the escape of human breast cancer cells in multiple models of obesity-associated breast cancer.

Keywords—Triple-negative breast cancer, Hypertrophy, Microphysiological system, Tumor engineering, Fat, Microvascular tissue engineering, Intravasation.

Address correspondence to Celeste M. Nelson, Department of Chemical and Biological Engineering, Princeton University, 303 Hoyt Laboratory, 25 William Street, Princeton, NJ 08544, USA; Joe Tien, Department of Biomedical Engineering, Boston University, 44 Cummington Mall, Boston, MA 02215, USA. Electronic mails: celesten@princeton.edu, jtien@bu.edu

ABBREVIATIONS

ASC	Adipose-derived stem cell
BMI	Body mass index
CM	Conditioned medium
ECM	Extracellular matrix
FFA	Free fatty acid
IFP	Interstitial fluid pressure
SMA	Smooth muscle actin
SVF	Stromal-vascular fraction

INTRODUCTION

Obesity plays detrimental roles in breast cancer and is a risk factor for breast cancer in both pre- and post-menopausal women.^{6,42} Obesity and its sequelae elevate the risk of breast cancer via characteristic adipose tissue expansion and remodeling, adipocyte hypertrophy, insulin resistance, low-grade inflammation, and metabolic dysfunction.^{12,44} Obesity-associated inflammation of adipose tissue is driven by upregulated expression of multiple cytokines including tumor necrosis factor- α , interleukin-6, and interleukin-1 β ,^{23,25} and leads to recruitment of macrophages in crown-like structures around dying adipocytes.⁸ These adipose tissue macrophages are pro-tumorigenic; for instance, obesity-associated macrophages promote expression of stem cell markers and increase tumor incidence in mouse models of triple-negative breast cancer.⁵³

Obesity also promotes breast cancer progression. Obese patients have poorer prognoses and more frequent distant metastases after relapse than non-obese patients do.³⁵ Diet-induced obesity also enhances tumor growth and formation of metastases in mouse models.⁵ These effects of obesity are mediated in part by changes in stromal cells. For example, obesity-associated senescent macrophages induce adipose stem cell (ASC)-mediated fibrosis,⁴⁵ and fibrosis is associated with breast cancer metastasis.¹⁰ Mobilization of free fatty acids (FFAs) from adipocytes increases the proliferation and migration of cancer cells, especially in obese conditions.^{3,56} Obesity-associated ASCs promote tumor growth and tumor cell migration by depositing fibronectin and increasing the activity of matrix metalloproteinases.^{34,47} Conditioned medium (CM) from obese donor-derived stromal-vascular fraction (SVF) cells or adipocytes increases the proliferation of MCF-7 human breast cancer cells, compared to CM from lean donor-derived cells.¹³ Obesity-associated neutrophils promote the extravasation of breast cancer cells by weakening endothelial intercellular adhesion.³⁹

Although past studies have identified how obesity impacts breast cancer at early and late stages of progression, the intermediate step between local invasion and intravasation (i.e., just before vascular dissemination) remains poorly understood. Various signals can control different stages of metastasis; moreover, the same perturbation can exert opposite effects at different stages.^{19,41} Thus, the effects of a given condition, such as obesity, on this intermediate stage cannot simply be extrapolated from studies of early or late stages of breast cancer progression. In prior work, we designed a 3D microfluidic model of a human breast microtumor adjacent to an empty, blind-ended, lymphatic vessel-like cavity within an adipose stroma.¹⁴ This model was developed to enable tumor cells to invade through an adipose stroma and “escape” into the lymphatic-like cavity, processes that resemble local invasion and intravasation in human breast cancer. This engineered model revealed that adipocytes and ASCs hasten the escape of malignant breast cancer cells via adipose cell-secreted soluble factors.

Since the ASCs that we used in the prior study were isolated from severely obese donors, a natural question is whether obesity *per se* plays a role in adipose cell-induced escape of breast cancer cells. For instance, does the body mass index (BMI) of the donor from which adipocytes and/or ASCs are derived correlate with invasion and/or escape? Does adipocyte hypertrophy, a hallmark of obesity, impact the rate of invasion or escape? This study investigates whether

obesity and its associated cellular changes affect adipose cell-induced escape of human breast cancer cells.

MATERIALS AND METHODS

Cell Culture

Green fluorescent protein (GFP)-expressing MDA-MB-231 human breast carcinoma cells (GFP-231 cells; Angio-Proteomie) were cultured at 37 °C and 5% CO₂ in tumor medium (TM), which consisted of DMEM/F12 (Hyclone) that was supplemented with 10% heat-inactivated fetal bovine serum (FBS, lot #B18020; Atlanta Biologicals) and 50 µg/mL gentamicin (Sigma). These cells were routinely passaged every 3–4 days through passage fifteen.

Human breast-derived ASCs from the Mayo Clinic Comprehensive Cancer Center and the Boston Nutrition Obesity Research Center (BNORC) were grown from the SVF of breast adipose tissue. With Institutional Review Board (IRB) approval and oversight, the Mayo Clinic Comprehensive Cancer Center identified women between the ages of 18 and 50 who were undergoing breast surgery. Potential participants who met the Mayo Clinic’s inclusion criteria were approached by the study coordinator during their preoperative appointment and were provided information about the study and procedures. Participants were allowed to ask questions and signed the consent form. This research used breast tissue that was retrieved after surgery but was deemed unnecessary for diagnostic reasons by the pathologist. With IRB approval and oversight, BNORC collected breast tissue from donors who underwent bilateral reduction mammoplasty. BNORC donors were excluded if they displayed a lack of English language skills, a disability that prevented informed consent, were less than 18 years of age, or were diagnosed with cancer or infections.

ASCs were differentiated using complete differentiation medium (CDM) and maintained using maintenance medium (MM), as described previously.^{14,32} ASCs were isolated from a total of eleven de-identified donors: four lean (BMI < 25), five obese (BMI ≥ 30), and two overweight (25 ≤ BMI < 30; Supplementary Table 1). ASCs were not pooled from multiple donors before use. ASCs that were differentiated and maintained for a total of 17–28 days were used for experiments that required adipocytes. We refer to these differentiated cultures as “adipose cells”; they consist of adipocytes and residual undifferentiated ASCs. Undifferentiated cells may also be breast-derived fibroblasts, myofibroblasts, or other mesenchymal cells that are morphologically indistinguishable from ASCs

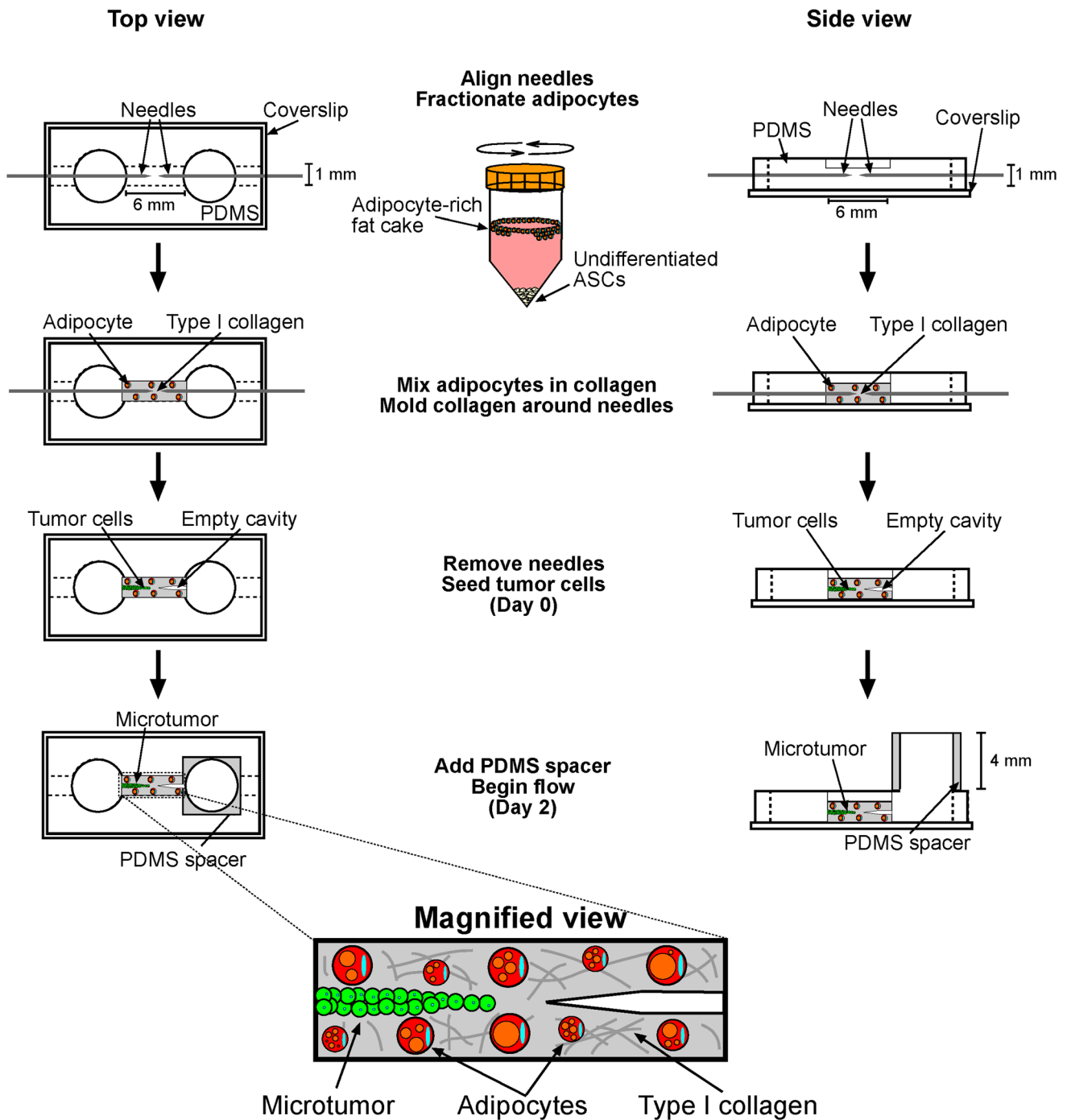


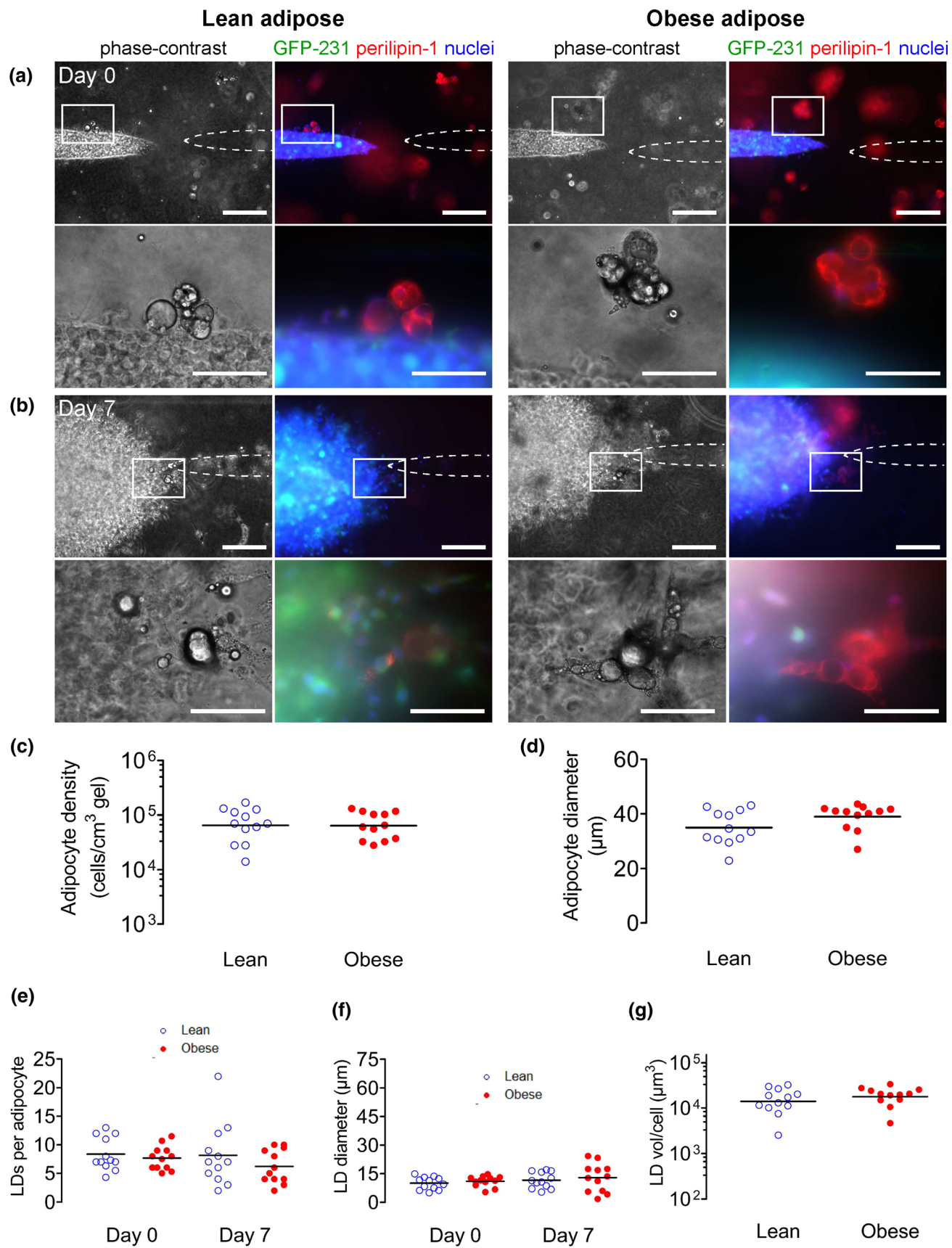
FIGURE 1. Schematic illustration of the approach used to engineer a 3D human breast microtumor and an empty cavity within a stroma containing human breast adipocytes.

(Fig. S1). All adipocytes used in this study were differentiated from ASCs in culture.

Preparation of Hypertrophic Adipocytes

Sodium oleate (Sigma) was dissolved in 10% fatty acid-free BSA (FAF-BSA; EMD Millipore) at 37 °C with rigorous stirring, passed through a sterile syringe

filter (0.2 μm ; Corning), and stored at -80 °C. The fatty acid solution (4 mM) was then diluted in CDM or MM to obtain a final concentration of 0.4 mM. Hypertrophic adipocytes were prepared by differentiating ASCs in oleate-containing CDM and MM. Control adipocytes were prepared by differentiating ASCs in CDM and MM that contained FAF-BSA without oleate.



◀ **FIGURE 2.** Phase-contrast and immunofluorescence images of GFP-expressing microtumors (green) in collagen gels laden with adipocytes that were differentiated from lean or obese donor-derived ASCs. Samples were stained for perilipin-1 (red) and nuclei (blue) on (a) day 0 and (b) day 7 after seeding and imaged at 10× and 63× magnification. Magnified images refer to the boxed areas in the row above. Images are from microtumors with initial tumor-to-cavity distances of (a) 129 μm (lean) and 111 μm (obese), and (b) 123 μm (lean) and 128 μm (obese). Scale bars refer to 250 μm (first row, third row) and 75 μm (second row, fourth row). (c) Adipocyte densities. (d) Adipocyte diameters. (e) Adipocyte locularity. (f) Lipid droplet diameters. (g) Lipid droplet volume per adipocyte. Each data point in (c)–(g) refers to the average value for the stroma of a single tumor sample. Graphical bars in (c) and (g) indicate geometric means. Graphical bars in (d)–(f) indicate arithmetic means. LD lipid droplet.

Formation of Engineered Microtumors

Microtumors ($n = 198$) were formed by modification of published needle-based techniques.^{14,43,51} For each tumor, we molded two opposing 120-μm-diameter blind-ended cavities that were separated by less than 200 μm (range 58–186 μm) in type I collagen gels at pH 7 (Fig. 1). Confluent cultures of breast adipose cells were treated with collagenase (1 mg/mL in HBSS; Worthington Biochemical) for 1 h, trypsinized, detached from the dish using MM that was supplemented with 3% FBS (MM+), and centrifuged at 500× g for 5 min. Residual collagenase was removed by washing the cells with MM+ and centrifuging once more. Bovine dermal type I collagen (4.9 mg/mL, acid-extracted and not pepsin-treated, lot #210090; Koken) was neutralized to pH 7 using 0.2 M NaOH and diluted with 10× HBSS (Gibco), water, and MM+ to obtain a collagen concentration of 3.9 mg/mL and an FBS concentration of 0.1%. For tumors in adipocyte-laden collagen gels, 8 μL of the floating “fat cake” that remained after centrifugation was added to 200 μL neutralized collagen to obtain a final density of 10^4 – 10^5 adipocytes/mL, depending on the average adipocyte size. For tumors in cell-free collagen gels, 8 μL of MM+ was added to 200 μL neutralized collagen. In all conditions, the final concentration of collagen was 3.75 mg/mL and the final concentration of FBS was $\leq 0.2\%$. Approximately 10 μL of collagen solution was transferred into each PDMS chamber. After 25 min of polymerization at 37 °C, MM+ was added to each well alongside the gel. The needles were removed after at least thirty more minutes to form two opposing blind-ended cavities. GFP-231 cells were added to one well and flowed into one cavity to form a densely packed “microtumor”. Starting on day 0 (i.e., the day on which tumor cells were seeded), microtumors were refed twice per day for up to 16 days using MM+, as in previous work.¹⁴

In some adipocyte-free collagen gels, undifferentiated ASCs (6×10^4 cells/mL) from a lean or obese donor were co-seeded with GFP-231 cells (1×10^6 cells/mL) into one cavity to form ASC-admixed tumors. The ASCs were obtained by treating undifferentiated confluent cultures with collagenase for one hour before trypsinizing, centrifuging, washing, and collecting pelleted cells. ASC-admixed tumors were refed twice per day for up to sixteen days using MM+.

Assessment of Tumor Invasion and Escape

Phase-contrast images were acquired daily using an Axiovert 200 inverted microscope (Zeiss), 10×/0.30 NA Plan-Neofluar objective, and an Axiocam MRm camera (Zeiss) at 1388 × 1040 resolution. Tumor-to-cavity distances were calculated as described previously,¹⁴ except that the difference in height was corrected by a factor of 1.358 (instead of 1.33) to account for the index of refraction of the culture medium.⁵⁵

We used phase-contrast imaging and fluorescence imaging to determine the first instances of invasion, when at least one tumor cell body was observed ≥ 20 μm from the initial microtumor, and escape, when at least one tumor cell body entered the adjacent blind-ended cavity.^{14,52} Microtumors that had not escaped by day 16 were discarded and censored on day 16 in Kaplan–Meier analysis. All experimental lean and obese donor-derived comparisons were repeated using ASCs from at least two different lean donors and two different obese donors. All hypertrophic comparisons were repeated using two different overweight donors.

Measurement of Adipocyte Parameters

Adipocyte diameter was defined as the maximum width of a given adipocyte on day 0. Lipid droplet diameters were measured on day 0 and day 7 at the adipocyte midplane. Adipocyte locularity was defined as the number of lipid droplets per adipocyte and was measured on day 0 and day 7. Parameters were measured using Axiovision ver. 4.8 (Zeiss). A morphometric technique was used to calculate the lipid droplet volume per adipocyte on day 0 from the lipid droplet area fraction.¹

Measurement of Collagen Permeability

Adipocyte-laden (10^4 – 10^5 cells/mL, depending on the degree of adipocyte hypertrophy) or cell-free collagen gels were subjected to a hydrostatic pressure drop of ~ 15 mm H₂O for 1.5–2 h by using ~ 1.5 -cm-high PDMS spacers that were filled with TM (viscosity of 0.72 cP at 37 °C). Darcy permeability (k) was cal-

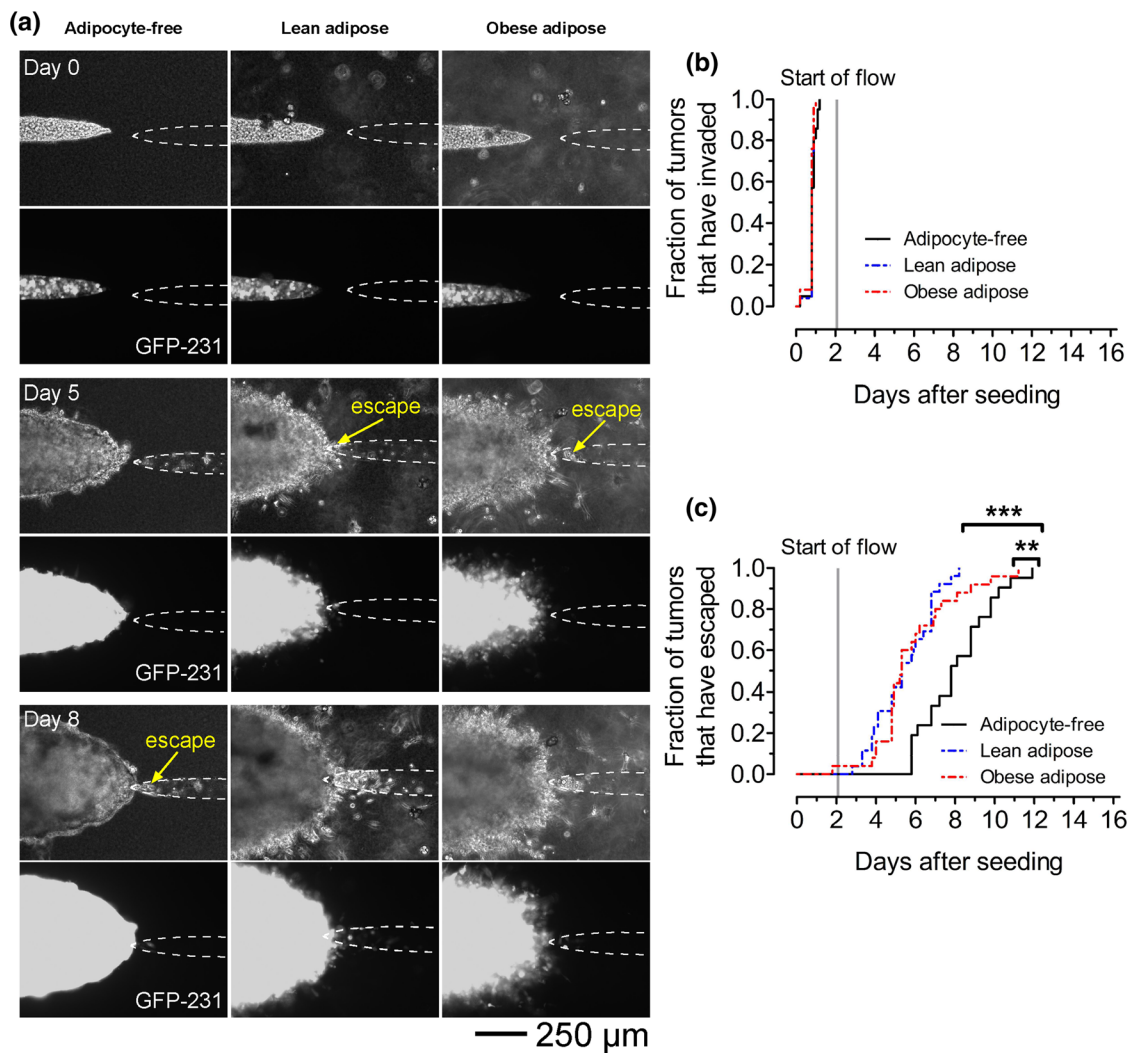


FIGURE 3. Adipocytes that are differentiated from breast-derived ASCs of lean and obese donors hasten escape to similar extents. (a) Time-lapse phase-contrast and fluorescence images of microtumors in adipocyte-free collagen gels and in lean and obese donor-derived adipose stroma. Images are from microtumors with initial tumor-to-cavity distances of 133 μm (adipocyte-free), 105 μm (lean), and 133 μm (obese). Kaplan–Meier curves of (b) invasion and (c) escape for microtumors in adipocyte-free collagen gels and in lean and obese donor-derived adipose stroma. ** $p < 0.01$; *** $p < 0.001$.

culated on day 2, 4, and 6 by measuring the flow rate across the gels, as described previously.¹⁴

Immunofluorescence Staining

Microtumors in adipocyte-laden collagen were stained using a protocol from prior work.^{14,43} All staining steps added 80 μL of solution to the well adjacent to the tumor and 20 μL of solution to the opposite well. Samples were fixed on day 0 or day 7 using 4% paraformaldehyde (PF; Electron Microscopy Sciences) in PBS for 15 min at room temperature, permeabilized using blocking buffer (BB) that consisted of 0.2% Triton X-100 (Sigma) and 5% goat serum (Invitrogen) in PBS for one hour, and labeled using a rabbit polyclonal antibody to perilipin-1 (5 $\mu\text{g}/$

mL in BB; Invitrogen) overnight at 4 $^{\circ}\text{C}$. The following day, samples were washed three times for 20 min each with BB. Alexa Fluor 594-conjugated goat anti-rabbit secondary antibody (5 $\mu\text{g}/\text{mL}$ in BB; Invitrogen) and Hoechst 33342 (1 $\mu\text{g}/\text{mL}$ in BB; Invitrogen) were then added simultaneously for one hour at room temperature. Washing was repeated with PBS three times for 20 min each.

In other experiments, undifferentiated ASCs from lean and obese donors were cultured on glass coverslips and fixed using 4% PF for 15 min at room temperature, permeabilized for one hour using BB, and stained using an Alexa Fluor 488-conjugated mouse monoclonal antibody to α -smooth muscle actin (αSMA ; clone 1A4, 0.5 $\mu\text{g}/\text{mL}$ in BB; Invitrogen) overnight at 4 $^{\circ}\text{C}$. The following day, cells were wa-

shed with BB three times for 20 min each, stained with Hoechst 33342 (1 $\mu\text{g}/\text{mL}$ in BB), and washed with PBS three more times for 20 min each.

Fluorescence images were acquired using an Axiovert 200 inverted microscope, 10 \times /0.30 *NA* Plan-Neofluar or 63 \times /0.95 W Achroplan water-immersion objective, and an Axiocam MRm camera at 1388 \times 1040 resolution.

Statistics

All statistical comparisons were performed in Graphpad Prism ver. 6. Kaplan–Meier curves of invasion or escape were compared using the log-rank (Mantel-Cox) test. The Kolmogorov–Smirnov test was used to compare cumulative frequency distributions for the starting tumor-to-cavity distance. Adipocyte densities, adipocyte diameters, lipid droplet volume per adipocyte, and the percentage of ASCs that were positive for αSMA were each compared using the Mann–Whitney *U* test. Measurements of adipocyte locularity, lipid droplet diameter, and Darcy permeability were each compared using two-way ANOVA. A *p* value of less than 0.05 was considered statistically significant in comparisons with two conditions. In datasets with three pairwise comparisons, the reported *p* values are Bonferroni-adjusted and should also be compared to a threshold of 0.05. BMI data are summarized as means \pm SD.

RESULTS

Engineering Microtumors in Lean and Obese Donor-Derived Adipocyte-Laden Stroma

Previously, we found that adipocytes and ASCs promote the invasion and escape of a microtumor composed of MDA-MB-231 human breast cancer cells.¹⁴ In that work, the ASCs were derived from the subcutaneous tissue of severely obese (BMI 41.1 \pm 2.0) donors who underwent bariatric surgery, and the vast majority (92%) of the cells in differentiated cultures were adipocytes.

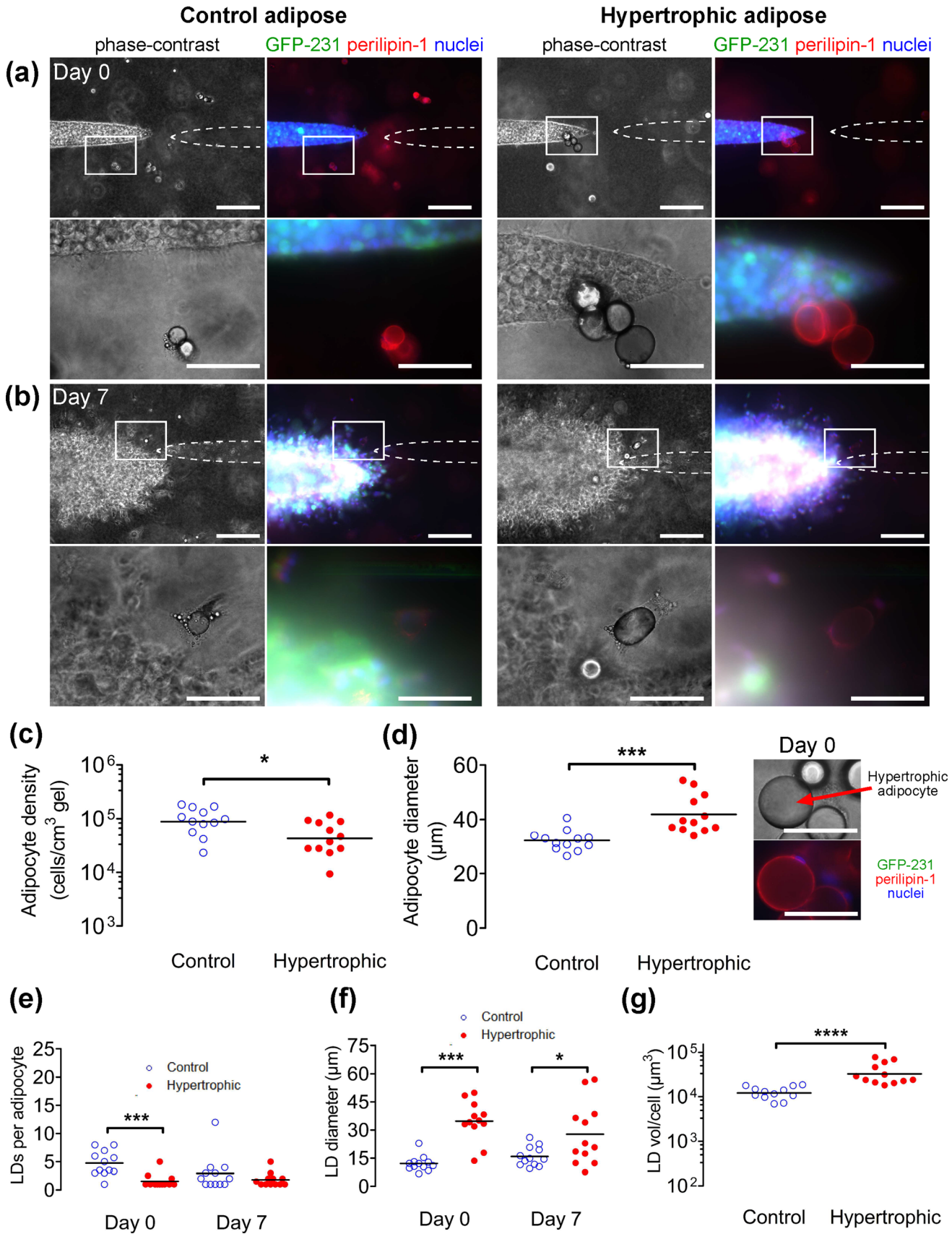
To determine whether the obesity status of the donors was responsible for the enhanced invasion and escape of breast cancer cells, we engineered tumors of MDA-MB-231 cells in either lean or obese donor-derived adipocyte-laden stroma (Fig. 2). Unlike in previous work, the tumor cells used here constitutively expressed GFP, which aided in assessing when invasion and escape occurred. We obtained ASCs from the breast tissue of either lean (BMI 23.4 \pm 2.1) or severely obese (BMI 39.2 \pm 2.5) donors (Supplementary Table 1). ASC cultures that were derived from lean and

obese donors contained comparable percentages of αSMA -positive myofibroblasts (18.8% in lean vs. 25.6% in obese, *p* = 0.39; Fig. S1). Compared to the subcutaneous abdominal ASCs that we used previously, breast-derived ASCs differentiated less efficiently. Whether the breast-derived ASCs were from lean or obese donors, only 32–36% of the cells in the differentiated adipose cultures were adipocytes. Since the differentiation of breast-derived ASCs was incomplete, we fractionated the differentiated cultures by centrifugation and only used floating cells from the adipocyte-rich fat cake to engineer adipocyte-laden stroma largely devoid of undifferentiated cells (Fig. 1).

GFP-expressing microtumors in either lean or obese donor-derived adipocyte-laden stroma were fixed on day 0 and day 7 after seeding and characterized using phase-contrast microscopy and immunofluorescence staining (Fig. 2a, b). Adipocytes were stained for perilipin-1, and all nuclei were counterstained using Hoechst 33342. Perilipin-1-negative stromal cells were considered to be residual (undifferentiated) ASCs or other mesenchymal cells. Lean and obese donor-derived stroma contained adipocytes of similar starting densities ($\sim 5 \times 10^4$ cells/cm³, *p* = 0.86; Fig. 2c) and diameters (~ 35 μm , *p* = 0.11; Fig. 2d). Both lean and obese donor-derived adipocytes were mostly multilocular and contained a comparable number of lipid droplets per cell (~ 7 per cell, *p* = 0.21; Fig. 2e) and similar lipid droplet diameters (~ 10 μm , *p* = 0.40; Fig. 2f) on day 0 and day 7. Lean and obese donor-derived adipocytes also had similar lipid droplet volumes per cell on day 0 ($\sim 10^4$ $\mu\text{m}^3/\text{cell}$, *p* = 0.31; Fig. 2g), and lean and obese donor-derived adipose stroma were each composed of $\sim 0.1\%$ lipid by volume fraction.

Lean and Obese Donor-Derived Adipose Stroma Hasten Escape Equally

Microtumors in adipocyte-free collagen primarily formed short, multicellular invasions that were often engulfed by the parent tumor as it grew (Fig. 3a, *left*). Microtumors in lean or obese adipose stroma formed both single-cell and long, multicellular invasions that remained connected to the parent tumor (Fig. 3a, *middle* and *right*). All microtumors had comparable tumor-to-cavity distances on day 0 (*p* = 0.60–0.78 for pairwise comparisons; Fig. S2a). Previously, we found that embedding adipose cells in collagen gels led to a modest increase in the average Darcy permeability of the ECM, with negligible changes in indentation modulus.^{14,33} Similarly, we found here that adding lean or obese donor-derived adipocytes to the collagen gels resulted in a slightly larger ($\sim 30\%$) permeability (*p* < 0.0003 for cell-free vs. lean and *p* = 0.0003 for



◀ **FIGURE 4.** Phase-contrast and immunofluorescence images of microtumors (green) in control or hypertrophic adipose stroma. Samples were stained for perilipin-1 (red) and nuclei (blue) on (a) day 0 and (b) day 7 and imaged at 10 \times and 63 \times magnification. Magnified images refer to the boxed areas in the row above. Images are from microtumors with initial tumor-to-cavity distances of (a) 110 μm (control) and 103 μm (hypertrophic), and (b) 132 μm (control) and 123 μm (hypertrophic). Scale bars refer to 250 μm (first row, third row) and 75 μm (second row, fourth row). (c) Adipocyte densities. (d) Adipocyte diameters. Inset shows hypertrophic adipocytes on day 0. Scale bar denotes 75 μm . (e) Adipocyte locularity. (f) Lipid droplet diameters. (g) Lipid droplet volume per adipocyte. Each data point in (c)–(g) refers to the average value for the stroma of a single tumor sample. Graphical bars in (c) and (g) indicate geometric means. Graphical bars in (d)–(f) indicate arithmetic means. * $p < 0.05$; *** $p < 0.001$; **** $p < 0.0001$. LD lipid droplet.

cell-free vs. obese; Fig. S3a). Assuming that ECM permeability scales as the square of pore size,²⁸ these changes in permeability are equivalent to a modest (~ 14%) increase in average pore size. The permeabilities of the adipocyte-laden gels under lean and obese conditions were not significantly different ($p = 1.0$).

In previous work, we found that an obese adipose stroma (derived from subcutaneous abdominal ASCs) hastens invasion and escape.¹⁴ Although the obese breast-derived stroma used here did not hasten invasion compared to tumors in adipocyte-free collagen ($p = 0.16$; Fig. 3b), it hastened the escape of microtumors [$p = 0.0072$, hazard ratio (HR) 2.8, 95% confidence interval (CI) 1.4–5.3; Fig. 3c]. Microtumors in lean breast-derived stroma also invaded at comparable rates to tumors in adipocyte-free collagen ($p = 0.25$; Fig. 3b). Surprisingly, they escaped sooner than microtumors in adipocyte-free collagen did ($p < 0.0003$, HR 5.6, 95% CI 2.7–11.6; Fig. 3c). Moreover, microtumors in lean adipose stroma invaded and escaped at similar rates to those in obese adipose stroma ($p = 1.0$ for both comparisons; Fig. 3b, c). Altogether, these results suggest that the obesity status of ASC donors does not appreciably alter the ability of adipocytes to enhance invasion or escape of human breast cancer cells.

Engineering Microtumors in Hypertrophic Adipose Stroma

One hallmark of obesity is hypertrophic growth of adipocytes. Hypertrophic adipocytes exhibit upregulated lipolysis and expression of inflammatory cytokines compared to normal adipocytes, which could affect the behavior of neighboring tumor cells.^{29,58} In our microtumors engineered within adipocyte-laden stroma, adipocytes from obese donor-derived ASCs were not hypertrophic: they were the same size as those

from lean donor-derived ASCs (Fig. 2d) and contained lipid droplets of similar size (Fig. 2f). This finding is perhaps not surprising, since cells may lose features characteristic of their native *in vivo* microenvironment when cultured *in vitro*.^{30,50}

These similarities in both adipocyte and lipid droplet size may have masked the effect of donor obesity on invasion or escape. To explore this possibility, we treated differentiated ASCs from overweight donors (BMI 27.8 ± 0.4) with medium that was supplemented with oleate, the most abundant fatty acid in human plasma and adipose tissue,^{24,40} or with FAF-BSA as a control. We then used the oleate-fed or control adipocytes to engineer tumors in hypertrophic or control adipose stroma, respectively (Fig. 4). These samples were fixed on day 0 and day 7 after seeding and characterized using phase-contrast microscopy and immunofluorescence analysis for perilipin-1 and nuclei (Figs. 4a, 4b).

As expected, adipose stroma that was engineered using oleate-fed adipocytes contained adipocytes of considerably larger diameters than control stroma did ($p = 0.0004$; Fig. 4d). The average diameter of these adipocytes was ~ 30% larger than that of control adipocytes, and some cells had diameters as large as ~ 60 μm . The oleate-fed adipocytes also had significantly fewer lipid droplets per cell than control adipocytes did on day 0 ($p < 0.001$; Fig. 4e). In fact, almost all oleate-treated adipocytes were unilocular (i.e., contained a single lipid droplet), whereas most control adipocytes were multilocular. Lipid droplets were significantly larger in oleate-treated adipocytes than in control adipocytes on day 0 ($p < 0.001$; Fig. 4f) and on day 7 ($p < 0.05$; Fig. 4f), and oleate-treated adipocytes had a greater total volume of lipid droplets per cell on day 0 ($p < 0.0001$; Fig. 4g). Thus, the oleate-treated adipocytes were hypertrophic. Consistent with its hypertrophy, the stroma of oleate-treated adipocytes had a lower adipocyte density than control adipose stroma did ($p = 0.028$; Fig. 4c). These phenotypic differences mimicked those *in vivo*, in which adipocyte hypertrophy is accompanied by a corresponding reduction in adipocyte density, while the lipid content (per volume of tissue) remains largely unchanged.^{37,46} Altogether, the combination of reduced locularity, larger lipid droplets, and lower cell density of the hypertrophic adipose stroma led to a lipid content comparable to that in the control adipose stroma (~ 0.1% lipid by volume fraction).

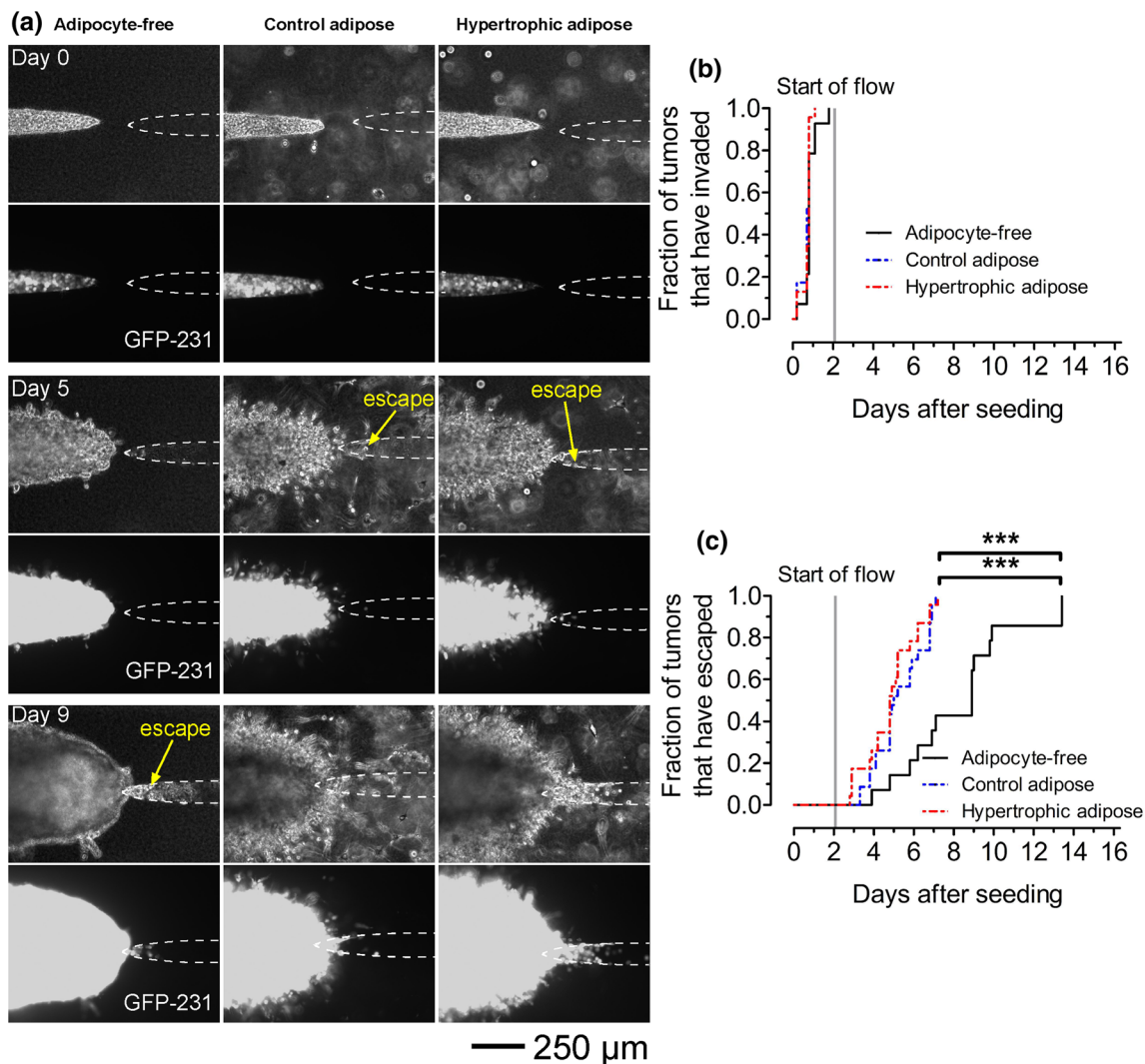


FIGURE 5. Control and hypertrophic adipose stroma each hasten escape. (a) Time-lapse phase-contrast and fluorescence images of microtumors in adipocyte-free collagen and in control and hypertrophic adipose stroma. Images are from microtumors with initial tumor-to-cavity distances of 124 μm (adipocyte-free), 106 μm (control), and 80 μm (hypertrophic). Kaplan–Meier curves of (b) invasion and (c) escape for microtumors in adipocyte-free collagen and in control and hypertrophic adipose stroma. *** $p < 0.001$.

Tumor Escape is Equally Hastened by Control and Hypertrophic Adipose Stroma

Microtumors in adipocyte-free collagen primarily formed multicellular invasions that were overtaken by the tumor aggregate (Fig. 5a, left). Microtumors in control and hypertrophic adipose stroma each formed single-cell and multicellular invasions (Fig. 5a, middle and right). All microtumors had comparable tumor-to-cavity distances on day 0 ($p = 0.65$ – 0.83 for pairwise comparisons; Fig. S2b). Control adipose stroma had a slightly larger ($\sim 22\%$) Darcy permeability than adipocyte-free gels did ($p = 0.0072$), while hypertrophic adipose stroma and adipocyte-free gels had similar

permeabilities ($p = 0.054$; Fig. S3b). No differences in Darcy permeability were detected between control and hypertrophic adipose stroma ($p = 1.0$). Microtumors in both control and hypertrophic adipose stroma invaded the ECM at similar rates as microtumors in adipocyte-free collagen did ($p = 0.093$ for control adipose stroma vs. adipocyte-free collagen and $p = 0.35$ for hypertrophic adipose stroma vs. adipocyte-free collagen; Fig. 5b). On the other hand, tumors in control and hypertrophic adipose stroma both escaped sooner than microtumors in adipocyte-free collagen did ($p < 0.0003$ for control adipose stroma vs. adipocyte-free collagen, HR 5.2, 95% CI 2.3–11.5 and $p < 0.0003$ for hypertrophic adipose stroma vs. adipocyte-free collagen, HR 5.9, 95% CI 2.6–13.2;

Fig. 5c). Microtumors in both forms of adipose stroma invaded and escaped at comparable rates ($p = 0.98$ for invasion and $p = 1.0$ for escape; Figs. 5b, 5c). These results suggest that the hypertrophy of adipocytes *per se* does not affect their ability to promote the invasion or escape of breast cancer cells.

Microtumor Invasion and Escape are Hastened by ASCs of Either Lean or Obese Donors

Since we did not detect any obesity-associated effects of adipocytes on tumor escape, we considered whether ASCs, the other key cell type that resides in adipose tissue, exerted obesity-dependent effects on escape (Fig. 6). Our prior study revealed that ASCs are a more potent source of escape-enhancing soluble factors than adipocytes are.¹⁴ Previous work by Fischbach and colleagues has also linked obesity-associated ASCs to increased breast cancer cell invasion, in part via direct contact between ASCs and tumor cells.^{34,47} To assess whether placing ASCs in direct contact with tumor cells leads to obesity-associated escape, we engineered mixed aggregates of tumor cells and ASCs that were isolated from a lean or obese donor; these ASC-admixed tumors were formed in cell-free collagen gels (Fig. 6a). All microtumors had matched initial tumor-to-cavity distances ($p = 0.76$ – 0.95 for pairwise comparisons; Fig. S2c). Consistent with previous findings, ASC-free (control) microtumors produced multicellular invasions (Fig. 6b, *left*). Microtumors that contained lean or obese donor-derived ASCs formed many single-cell and long, multicellular invasions that extended far beyond the parent tumor into the collagen gel (Fig. 6b, *middle, right*).

Consistent with the results described above for tumors that were formed within a spatially distinct adipose stroma (Figs. 3, 5), microtumors with ASCs embedded within the tumor itself invaded at similar rates regardless of the obesity status of the ASC donor ($p = 1.0$; Fig. 6c). Invasion was hastened by both lean and obese donor-derived ASCs when compared to ASC-free microtumors ($p < 0.0003$ for lean ASC-admixed vs. ASC-free tumors, HR 10.9, 95% CI 3.5–33.9 and $p < 0.0003$ for obese ASC-admixed vs. ASC-free tumors, HR 10.6, 95% CI 3.4–33.7). Both lean and obese ASC-admixed tumors also promoted escape ($p = 0.0015$ for lean ASC-admixed vs. ASC-free tumors, HR 5.0, 95% CI 2.0–12.5 and $p = 0.0036$ for obese ASC-admixed vs. ASC-free tumors, HR 4.9, 95% CI 1.9–12.9; Fig. 6d). Invading and escaping tumor cells in both types of ASC-admixed tumors were primarily led by the ASCs, which did not express GFP (Fig. 6e). Consistent with the experiments in which the microtumor and adipocytes were compartmentalized, microtumors in which tumor cells were in direct con-

tact with either lean or obese donor-derived ASCs escaped at comparable rates ($p = 1.0$; Fig. 6d). These results suggest that the obesity status of ASC donors does not modify the effects of ASC-induced invasion or escape.

DISCUSSION

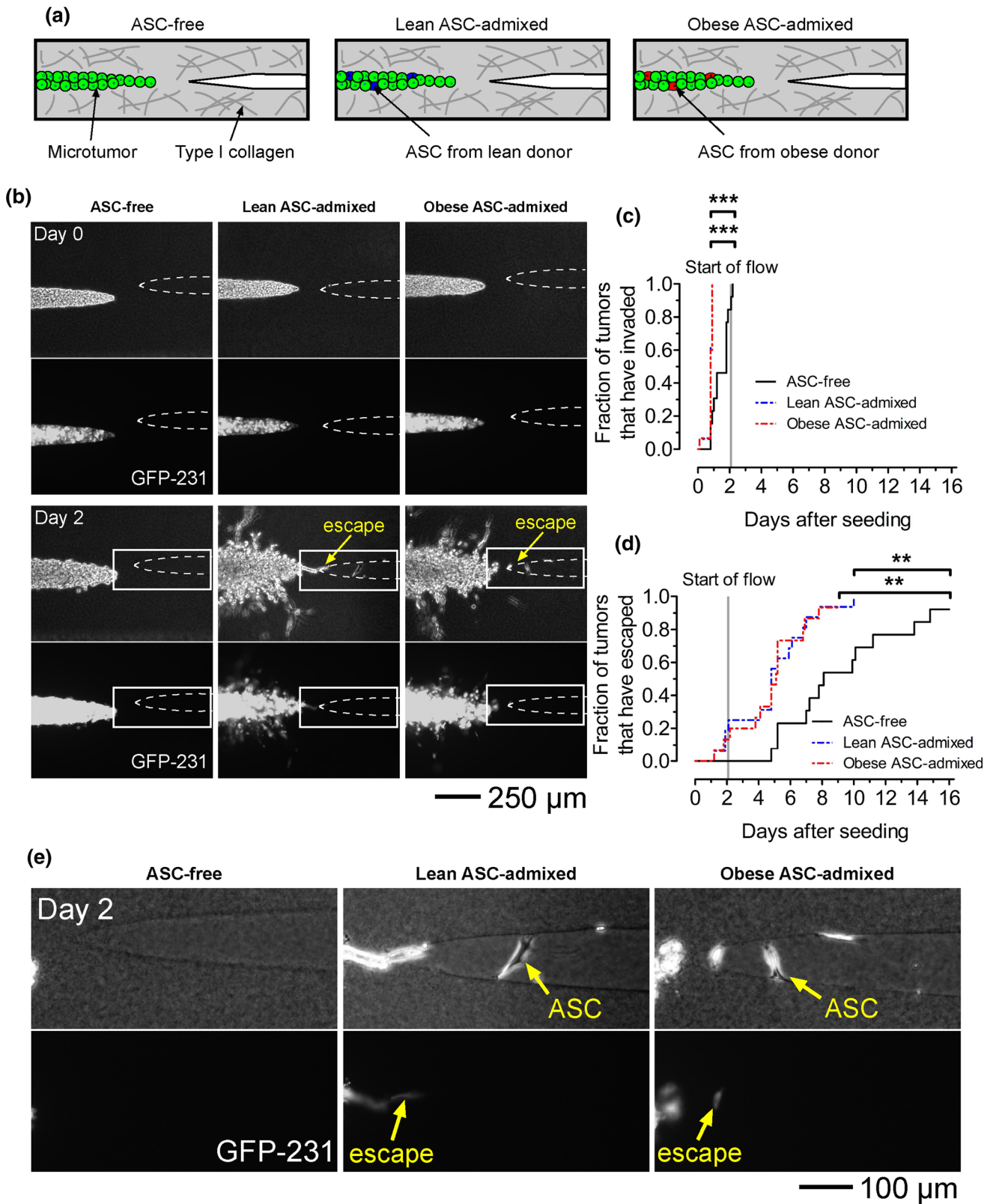
Summary of Findings

The central—and to us, quite unexpected—result of the current study is that the obesity status of adipose cells has little-to-no effect on the invasion or escape of human breast cancer cells. Guided by several past studies that have shown a correlative and/or causal relationship between obesity and breast cancer initiation and metastasis,^{4,15,38} we expected to find in our engineered models that obesity-associated adipose cells would promote more breast cancer cell escape than lean/control adipose cells would. Yet, in three distinct models of obesity—one that uses adipocytes differentiated from obese donor-derived ASCs, one that mimics adipose hypertrophy by loading the adipocytes with oleate, and one that incorporates obese donor-derived ASCs directly into the tumor—the presence of the obesity-associated factors did not promote invasion or escape. Instead, we consistently found increased escape (and in some cases, increased invasion) when comparing the behavior of tumors with and without adipose cells, regardless of the obesity status of those adipose cells.

More precisely, the BMI of the ASC donor and the degree of adipocyte hypertrophy had no effect on the kinetics of escape. Below, we consider the implications of these surprising findings and the potential relevance to breast cancer progression.

Engineered Models of Obesity-Associated Adipose Tissue

Previously, we engineered a microscale breast cancer model in which the stroma contained adipose cells that were derived from subcutaneous abdominal ASCs of obese donors.¹⁴ That work compared the behavior of tumors in cell-free vs. adipose stroma and revealed that the presence of adipose cells (which were solely from obese donors) accelerates the escape of human breast cancer cells. In the current study, we sought to assess whether the obesity status of the adipose stroma modifies the rate of escape. We employed three strategies to mimic obesity *in vitro*: using obese donor-derived differentiated ASCs to engineer an obesity-associated adipose stroma, promoting adipocyte hypertrophy, and intermixing ASCs from obese donors



◀ **FIGURE 6. Lean and obese donor-derived ASCs in direct contact with tumor cells each hasten invasion and escape. (a) Schematic illustration of control or ASC-admixed microtumors adjacent to an empty cavity within a cell-free collagen gel. (b) Time-lapse phase-contrast and fluorescence images of ASC-free microtumors and microtumors that contain lean or obese donor-derived ASCs. Images are from microtumors with initial tumor-to-cavity distances of 108 μm (ASC-free), 106 μm (lean ASC-admixed), and 73 μm (obese ASC-admixed). Kaplan–Meier curves of (c) invasion and (d) escape for ASC-free microtumors and for microtumors that contain lean or obese donor-derived ASCs. (e) Magnified images of the boxed regions in (b). ** $p < 0.01$; *** $p < 0.001$.**

directly with tumor cells. It is important to assess to what extent these methods yield models that display known obesity-associated characteristics.

ASCs from lean (wild-type) and obese (*ob/ob*) mice have been reported to differ in their myofibroblast composition, with mammary fat pads of *ob/ob* mice having more αSMA -expressing ASCs.⁴⁷ In contrast, we detected similar fractions of myofibroblasts in lean and obese donor-derived ASC cultures. These differences may result from either species-specific or depot-specific differences between ASCs derived from mouse mammary tissue and those derived from human breast tissue. Upon differentiation, our resulting adipocytes from lean or obese donor-derived ASCs were multilocular and morphologically indistinguishable. The mean adipocyte diameter ($\sim 35 \mu\text{m}$) and lipid droplet diameter ($\sim 10 \mu\text{m}$) in our lean and obese adipose stroma were similar to the values from human adipocytes used in other 3D culture models,^{20,48,59} but were much smaller than those of native human adipocytes *in vivo*, especially in obese subjects. These observations motivated our strategy to mimic hypertrophy (a hallmark feature of obesity) *in vitro*, in which we supplied free fatty acid to enlarge the lipid droplets in adipocytes.⁹ We successfully generated hypertrophic human adipocytes using oleate treatment: these adipocytes had typical diameters of 45–50 μm (with some as large as 60 μm), were predominantly unilocular, and contained lipid droplets ($\sim 35 \mu\text{m}$ diameter) that were notably larger than those in our control adipocytes and in adipocytes in previously published work.^{9,27,48} In fact, our oleate-fed adipocytes were comparable in size to lean human adipocytes observed *in vivo*.^{46,54} The oleate-treated adipocytes were still smaller than adipocytes of obese humans *in vivo*, and extending the differentiation time may be able to bridge the size gap.^{17,26}

Despite differences in adipocyte size, the adipose tissues of lean and obese humans *in vivo* contain similar amounts ($\sim 100\%$ by volume) of lipid. Likewise, the lipid contents of our engineered control and hypertrophic adipose stromas were also matched, albeit at a

much lower level ($\sim 0.1\%$ lipid by volume). In principle, introducing a higher density of adipocytes into the collagen would increase the lipid content of our engineered adipose tissues. The density of adipocytes (10^4 – 10^5 cells/ cm^3 gel) in this study matched that of our prior work and permitted routine time-lapse imaging of the tumor cells as they invaded and escaped.¹⁴

How Obese Adipose Tissue Affects Breast Cancer Progression In Vitro

Regardless of how it was simulated *in vitro*, obesity had no effect on adipose-induced invasion or escape of human breast cancer cells. At first glance, this result appears to run counter to the work of Fischbach and co-workers, who used ASCs from genetically obese *ob/ob* mice to conclude that obesity-associated ASCs promote breast cancer cell invasion.^{34,47} Closer inspection, however, reveals several differences between our and Fischbach's studies that may account for the different results. First, and perhaps most importantly, we used ASCs from outbred obese humans, while the *ob/ob* mouse is inbred and lacks leptin. Notably, the vast majority of obese humans exhibit elevated levels of circulating leptin,^{2,11} and the degree to which these differences in leptin concentration *in vivo* contribute to the obesity-associated change in ASCs is unclear. Second, the studies with ASCs from *ob/ob* mice showed greater invasive area of human breast cancer cell spheroids and increased numbers of invading breast cancer cells, compared to cancer cell spheroids grown with wild-type ASCs. In contrast, our invasion assay notes the first instance of invasion instead of the total number of invasions or the total area that they occupy. Third, ASCs from *ob/ob* mice exert their effects on breast cancer cells through physical remodeling of the ECM, whereas ASCs from obese humans hasten breast cancer cell escape in large part through chemical signaling.^{14,34} Fourth, we note that signals that alter individual stages of breast cancer progression (e.g., invasion) do not necessarily promote subsequent stages (e.g., intravasation, extravasation) or metastasis.^{19,21,41} The studies of Fischbach and co-workers focused on invasion, while ours has included escape into a lymphatic-like cavity. Finally, one must always keep in mind the potential for species-specific effects in obesity.³¹

Other work has used *in vitro* models of adipocyte hypertrophy as a mimic of obesity and found that the enlargement of adipocytes enhances breast cancer cell proliferation and migration.³ To the best of our knowledge, our study is the first to engineer a 3D hypertrophic adipocyte-laden stroma through which human breast cancer cells can invade and subsequently escape. While the presence of embedded hypertrophic

adipocytes accelerated the rate of escape when compared to adipocyte-free collagen, non-hypertrophic adipose stroma also enhanced escape to a similar extent. Thus, our findings consistently show that obesity does not modify the rate at which adipose cells promote the escape of breast cancer cells, and these findings are not the result of using a tumor escape assay that is insensitive to differences in escape kinetics.

Implications for Breast Cancer Metastasis

Given that obesity is associated with poorer prognosis and metastasis in breast cancer, how do our findings fit with the existing understanding of the roles of obesity in breast cancer? One possibility is that obesity does not accelerate breast cancer metastasis at the intermediate stage of intravasation. This possibility is supported by our finding that neither obesity-specific adipose cells nor the hypertrophy of adipocytes modified the ability of adipose cells to promote escape of human breast cancer cells *in vitro*. Intriguingly, recent studies have shown that the presence of circulating tumor cells is not correlated with BMI in breast cancer patients,^{16,49} and that BMI is not correlated with lymphatic metastasis in human breast cancer.¹⁸

On the other hand, one must always keep in mind that *in vitro* models of disease do not capture the complete set of alterations that occur *in vivo*, especially when modeling a complex metabolic condition such as obesity. It is possible that a critical obesity-associated stromal cell or factor (e.g., an immune or inflammatory component) that alters escape is lacking in our models. For example, obesity is associated with recruitment of macrophages and their metabolic activation,^{7,36,57} and macrophages can accelerate intravasation.²² The development of breast cancer models that include immune or inflammatory components of the obese microenvironment will be needed to obtain a more complete understanding of the role of obesity in human breast cancer cell escape.

The tumor models used here and in our previous work have relied exclusively on the MDA-MB-231 human triple-negative breast cancer cell line. Whether obesity-associated factors would show similarly modest effects in other triple-negative breast cancer cell lines or in cell lines of luminal or other breast cancer subtypes is unknown, and addressing this question will await the engineering of tumor models from these other cell lines.

CONCLUSIONS

Although obesity can accelerate breast cancer progression, the complexity of the obese state—with simultaneous changes in adipocytes, ASCs, and other local cell populations within adipose tissue and in the systemic environment—has made a more detailed understanding of how obesity contributes to breast cancer challenging. Our development and use of an *in vitro* microscale breast cancer model in an adipose stroma that exhibits select aspects of obesity has shown that obesity-specific alterations in ASCs and adipocyte hypertrophy do not enhance the escape of triple-negative breast cancer cells into a lymphatic-like channel. Other characteristics of obesity *in vivo*, such as a low-grade inflammatory state that is accompanied by infiltration of macrophages into adipose tissue, were not represented in these models. Thus, it remains to be seen whether our results are indicative of a true marginal effect of obesity on the intermediate stages of breast cancer, or whether they arise from an inadequacy in this *in vitro* model of obesity in breast cancer. Future work will reproduce these other obesity-associated factors and use cells of other breast cancer subtypes to provide a wider assessment of the role of obesity in human breast cancer progression.

SUPPLEMENTARY INFORMATION

The online version contains supplementary material available at <https://doi.org/10.1007/s12195-022-00750-y>.

CONFLICT OF INTEREST

Yoseph W. Dance, Mackenzie C. Obenreder, Alex J. Seibel, Tova Meshulam, Joshua W. Ogony, Nikhil Lahiri, Laura Pacheco-Spann, Derek C. Radisky, Matthew D. Layne, Stephen R. Farmer, Celeste M. Nelson, and Joe Tien declare that they have no conflict of interest.

ETHICAL APPROVAL

All procedures followed were in accordance with the ethical standards of the responsible committee on human experimentation (institutional and national) and with the Helsinki Declaration of 1975, as revised in 2000. Informed consent was obtained from all patients for being included in the study.

ACKNOWLEDGMENTS

This work was supported by award U01 CA214292 from the National Cancer Institute and by award P30 DK046200 (Boston Nutrition Obesity Research Center; BNORC) from the National Institute of Diabetes and Digestive and Kidney Diseases. Y.W.D. was funded through the CURE Diversity Research Supplements Program at the National Cancer Institute, and M.C.O. was funded through the Undergraduate Research Opportunities Program at Boston University. Human breast-derived ASCs were provided by the Mayo Clinic Comprehensive Cancer Center and BNORC. We thank Miguel L. Batista, Jr. and Nabil Rabhi for insightful discussions.

REFERENCES

- ¹Aherne, W. A., and M. S. Dunnill. *Morphometry*. London: Arnold Publishers, pp. 1–205, 1982.
- ²Ahima, R. S., and J. S. Flier. Leptin. *Annu. Rev. Physiol.* 62:413–437, 2000.
- ³Balaban, S., R. F. Shearer, L. S. Lee, M. van Geldermalsen, M. Schreuder, H. C. Shtein, R. Cairns, K. C. Thomas, D. J. Fazakerley, T. Grewal, J. Holst, D. N. Saunders, and A. J. Hoy. Adipocyte lipolysis links obesity to breast cancer growth: adipocyte-derived fatty acids drive breast cancer cell proliferation and migration. *Cancer Metab.* 5:1, 2017.
- ⁴Barone, I., C. Giordano, D. Bonfiglio, S. Andò, and S. Catalano. The weight of obesity in breast cancer progression and metastasis: clinical and molecular perspectives. *Semin. Cancer Biol.* 60:274–284, 2020.
- ⁵Bousquenaud, M., F. Fico, G. Solinas, C. Rüegg, and A. Santamaria-Martínez. Obesity promotes the expansion of metastasis-initiating cells in breast cancer. *Breast Cancer Res.* 20:104, 2018.
- ⁶Calle, E. E., and R. Kaaks. Overweight, obesity and cancer: epidemiological evidence and proposed mechanisms. *Nat. Rev. Cancer* 4:579–591, 2004.
- ⁷Chakarov, S., C. Blériot, and F. Ginhoux. Role of adipose tissue macrophages in obesity-related disorders. *J. Exp. Med.* 219:e20211948, 2022.
- ⁸Cinti, S., G. Mitchell, G. Barbatelli, I. Murano, E. Ceresi, E. Faloia, S. Wang, M. Fortier, A. S. Greenberg, and M. S. Obin. Adipocyte death defines macrophage localization and function in adipose tissue of obese mice and humans. *J. Lipid Res.* 46:2347–2355, 2005.
- ⁹Collins, J. M., M. J. Neville, K. E. Pinnick, L. Hodson, B. Ruyter, T. H. van Dijk, D. J. Reijngoud, M. D. Fielding, and K. N. Frayn. De novo lipogenesis in the differentiating human adipocyte can provide all fatty acids necessary for maturation. *J. Lipid Res.* 52:1683–1692, 2011.
- ¹⁰Colpaert, C., P. Vermeulen, E. Van Marck, and L. Dirix. The presence of a fibrotic focus is an independent predictor of early metastasis in lymph node-negative breast cancer patients. *Am. J. Surg. Pathol.* 25:1557–1558, 2001.
- ¹¹Considine, R. V., M. K. Sinha, M. L. Heiman, A. Kriauciunas, T. W. Stephens, M. R. Nyce, J. P. Ohannessian, C. C. Marco, L. J. McKee, and T. L. Bauer. Serum immunoreactive-leptin concentrations in normal-weight and obese humans. *N. Engl. J. Med.* 334:292–295, 1996.
- ¹²Cozzo, A. J., A. M. Fuller, and L. Makowski. Contribution of adipose tissue to development of cancer. *Compr. Physiol.* 8:237–282, 2017.
- ¹³D’Esposito, V., F. Passaretti, A. Hammarstedt, D. Li-guoro, D. Terracciano, G. Molea, L. Canta, C. Miele, U. Smith, F. Beguinot, and P. Formisano. Adipocyte-released insulin-like growth factor-1 is regulated by glucose and fatty acids and controls breast cancer cell growth in vitro. *Diabetologia* 55:2811–2822, 2012.
- ¹⁴Dance, Y. W., T. Meshulam, A. J. Seibel, M. C. Obenreder, M. D. Layne, C. M. Nelson, and J. Tien. Adipose stroma accelerates the invasion and escape of human breast cancer cells from an engineered microtumor. *Cell. Mol. Bioeng.* 15:15–29, 2022.
- ¹⁵Ewertz, M., M. B. Jensen, K. Gunnarsdóttir, I. Højris, E. H. Jakobsen, D. Nielsen, L. E. Stenbygaard, U. B. Tange, and S. Cold. Effect of obesity on prognosis after early-stage breast cancer. *J. Clin. Oncol.* 29:25–31, 2011.
- ¹⁶Fayanju, O. M., C. S. Hall, J. B. Bauldry, M. Karhade, L. M. Valad, H. M. Kuerer, S. M. DeSnyder, C. H. Barcenas, and A. Lucci. Body mass index mediates the prognostic significance of circulating tumor cells in inflammatory breast cancer. *Am. J. Surg.* 214:666–671, 2017.
- ¹⁷Fischbach, C., T. Spruss, B. Weiser, M. Neubauer, C. Becker, M. Hacker, A. Göpferich, and T. Blunk. Generation of mature fat pads in vitro and in vivo utilizing 3-D long-term culture of 3T3-L1 preadipocytes. *Exp. Cell Res.* 300:54–64, 2004.
- ¹⁸Gao, Y., X. Chen, Q. He, R. C. Gimple, Y. Liao, L. Wang, R. Wu, Q. Xie, J. N. Rich, K. Shen, and Z. Yuan. Adipocytes promote breast tumorigenesis through TAZ-dependent secretion of resistin. *Proc. Natl. Acad. Sci. USA* 117:33295–33304, 2020.
- ¹⁹Grasset, E. M., M. Dunworth, G. Sharma, M. Loth, J. Tandurella, A. Cimino-Mathews, M. Gentz, S. Bracht, M. Haynes, E. J. Fertig, and A. J. Ewald. Triple-negative breast cancer metastasis involves complex epithelial-mesenchymal transition dynamics and requires vimentin. *Sci. Transl. Med.* 14:eabn7571, 2022.
- ²⁰Hammel, J. H., and E. Bellas. Endothelial cell crosstalk improves browning but hinders white adipocyte maturation in 3D engineered adipose tissue. *Integr. Biol.* 12:81–89, 2020.
- ²¹Hapach, L. A., S. P. Carey, S. C. Schwager, P. V. Taufalele, W. Wang, J. A. Mosier, N. Ortiz-Otero, T. J. McArdle, Z. E. Goldblatt, M. C. Lampi, F. Bordeleau, J. R. Marshall, I. M. Richardson, J. Li, M. R. King, and C. A. Reinhart-King. Phenotypic heterogeneity and metastasis of breast cancer cells. *Cancer Res.* 81:3649–3663, 2021.
- ²²Harney, A. S., E. N. Arwert, D. Entenberg, Y. Wang, P. Guo, B. Z. Qian, M. H. Oktay, J. W. Pollard, J. G. Jones, and J. S. Condeelis. Real-time imaging reveals local, transient vascular permeability, and tumor cell intravasation stimulated by TIE2^{hi} macrophage-derived VEGFA. *Cancer Discov.* 5:932–943, 2015.
- ²³Hildreth, A. D., F. Ma, Y. Y. Wong, R. Sun, M. Pellegrini, and T. E. O’Sullivan. Single-cell sequencing of human white adipose tissue identifies new cell states in health and obesity. *Nat. Immunol.* 22:639–653, 2021.
- ²⁴Hodson, L., C. M. Skeaff, and B. A. Fielding. Fatty acid composition of adipose tissue and blood in humans and its use as a biomarker of dietary intake. *Prog. Lipid Res.* 47:348–380, 2008.

- ²⁵Hotamisligil, G. S., N. S. Shargill, and B. M. Spiegelman. Adipose expression of tumor necrosis factor- α : direct role in obesity-linked insulin resistance. *Science* 259:87–91, 1993.
- ²⁶Hsiao, A. Y., T. Okitsu, H. Teramae, and S. Takeuchi. 3D tissue formation of unilocular adipocytes in hydrogel microfibers. *Adv. Healthc. Mater.* 5:548–556, 2016.
- ²⁷Ioannidou, A., S. Alatar, R. Schipper, F. Baganha, M. Åhlander, A. Hornell, R. M. Fisher, and C. E. Hagberg. Hypertrophied human adipocyte spheroids as in vitro model of weight gain and adipose tissue dysfunction. *J. Physiol.* 600:869–883, 2022.
- ²⁸Jackson, G. W., and D. F. James. The permeability of fibrous porous media. *Can. J. Chem. Eng.* 64:364–374, 1986.
- ²⁹Jernäs, M., J. Palming, K. Sjöholm, E. Jennische, P. A. Svensson, B. G. Gabrielsson, M. Levin, A. Sjögren, M. Rudemo, T. C. Lystig, B. Carlsson, L. M. Carlsson, and M. Lönn. Separation of human adipocytes by size: hypertrophic fat cells display distinct gene expression. *FASEB J.* 20:E832–E839, 2006.
- ³⁰Kitsis, R. N., and L. A. Leinwand. Discordance between gene regulation in vitro and in vivo. *Gene Exp.* 2:313–318, 1992.
- ³¹Kleinert, M., C. Clemmensen, S. M. Hofmann, M. C. Moore, S. Renner, S. C. Woods, P. Huypens, J. Beckers, M. H. de Angelis, A. Schürmann, M. Bakhti, M. Klingenspor, M. Heiman, A. D. Cherrington, M. Ristow, H. Lickert, E. Wolf, P. J. Havel, T. D. Müller, and M. H. Tschöp. Animal models of obesity and diabetes mellitus. *Nat. Rev. Endocrinol.* 14:140–162, 2018.
- ³²Lee, M. J., and S. K. Fried. Optimal protocol for the differentiation and metabolic analysis of human adipose stromal cells. *Methods Enzymol.* 538:49–65, 2014.
- ³³Li, X., J. Xia, C. T. Nicolescu, M. W. Massidda, T. J. Ryan, and J. Tien. Engineering of microscale vascularized fat that responds to perfusion with lipoactive hormones. *Biofabrication* 11:014101, 2019.
- ³⁴Ling, L., J. A. Mulligan, Y. Ouyang, A. A. Shimpi, R. M. Williams, G. F. Beeghly, B. D. Hopkins, J. A. Spector, S. G. Adie, and C. Fischbach. Obesity-associated adipose stromal cells promote breast cancer invasion through direct cell contact and ECM remodeling. *Adv. Funct. Mater.* 30:1910650, 2020.
- ³⁵Lohmann, A. E., S. V. Soldera, I. Pimentel, D. Ribnikar, M. Ennis, E. Amir, and P. J. Goodwin. Association of obesity with breast cancer outcome in relation to cancer subtypes: a meta-analysis. *J. Natl. Cancer Inst.* 113:1465–1475, 2021.
- ³⁶Lumeng, C. N., J. L. Bodzin, and A. R. Saltiel. Obesity induces a phenotypic switch in adipose tissue macrophage polarization. *J. Clin. Investig.* 117:175–184, 2007.
- ³⁷Martin, A. D., M. Z. Daniel, D. T. Drinkwater, and J. P. Clarys. Adipose tissue density, estimated adipose lipid fraction and whole body adiposity in male cadavers. *Int. J. Obes. Relat. Metab. Disord.* 18:79–83, 1994.
- ³⁸Mazzarella, L., D. Disalvatore, V. Bagnardi, N. Rotmensz, D. Galbiati, S. Caputo, G. Curigliano, and P. G. Pelicci. Obesity increases the incidence of distant metastases in oestrogen receptor-negative human epidermal growth factor receptor 2-positive breast cancer patients. *Eur. J. Cancer* 49:3588–3597, 2013.
- ³⁹McDowell, S. A. C., R. B. E. Luo, A. Arabzadeh, S. Doré, N. C. Bennett, V. Breton, E. Karimi, M. Rezanejad, R. R. Yang, K. D. Lach, M. S. M. Issac, B. Samborska, L. J. M. Perus, D. Moldoveanu, Y. Wei, B. Fiset, R. F. Rayes, I. R. Watson, L. Kazak, M. C. Guiot, P. O. Fiset, J. D. Spicer, A. J. Dannenberg, L. A. Walsh, and D. F. Quail. Neutrophil oxidative stress mediates obesity-associated vascular dysfunction and metastatic transmigration. *Nat. Cancer* 2:545–562, 2021.
- ⁴⁰Mehta, A., A. M. Oeser, and M. G. Carlson. Rapid quantitation of free fatty acids in human plasma by high-performance liquid chromatography. *J. Chromatogr. B Biomed. Sci. Appl.* 719:9–23, 1998.
- ⁴¹Padmanaban, V., I. Krol, Y. Suhail, B. M. Szczerba, N. Aceto, J. S. Bader, and A. J. Ewald. E-cadherin is required for metastasis in multiple models of breast cancer. *Nature* 573:439–444, 2019.
- ⁴²Pierobon, M., and C. L. Frankenfeld. Obesity as a risk factor for triple-negative breast cancers: a systematic review and meta-analysis. *Breast Cancer Res. Treat.* 137:307–314, 2013.
- ⁴³Piotrowski-Daspit, A. S., A. K. Simi, M. F. Pang, J. Tien, and C. M. Nelson. A 3D culture model to study how fluid pressure and flow affect the behavior of aggregates of epithelial cells. *Methods Mol. Biol.* 1501:245–257, 2017.
- ⁴⁴Quail, D. F., and A. J. Dannenberg. The obese adipose tissue microenvironment in cancer development and progression. *Nat. Rev. Endocrinol.* 15:139–154, 2019.
- ⁴⁵Rabhi, N., K. Desevin, A. C. Belkina, A. Tilston-Lunel, X. Varelas, M. D. Layne, and S. R. Farmer. Obesity-induced senescent macrophages activate a fibrotic transcriptional program in adipocyte progenitors. *Life Sci. Alliance* 5:e202101286, 2022.
- ⁴⁶Salans, L. B., S. W. Cushman, and R. E. Weismann. Studies of human adipose tissue. Adipose cell size and number in nonobese and obese patients. *J. Clin. Investig.* 52:929–941, 1973.
- ⁴⁷Seo, B. R., P. Bhardwaj, S. Choi, J. Gonzalez, R. C. Andresen Eguiluz, K. Wang, S. Mohanan, P. G. Morris, B. Du, X. K. Zhou, L. T. Vahdat, A. Verma, O. Elemento, C. A. Hudis, R. M. Williams, D. Gourdon, A. J. Dannenberg, and C. Fischbach. Obesity-dependent changes in interstitial ECM mechanics promote breast tumorigenesis. *Sci. Transl. Med.* 7:301ra130, 2015.
- ⁴⁸Shen, J. X., M. Couchet, J. Dufau, T. de Castro Barbosa, M. H. Ulbrich, M. Helmstädter, A. M. Kemas, R. Zandi Shafagh, M. A. Marques, J. B. Hansen, N. Mejhert, D. Langin, M. Rydén, and V. M. Lauschke. 3D adipose tissue culture links the organotypic microenvironment to improved adipogenesis. *Adv. Sci.* 8:e2100106, 2021.
- ⁴⁹Shi, Y., G. Zhang, Y. Wang, C. Ren, L. Wen, W. Zhu, X. Chen, and N. Liao. Presence of circulating tumor cells is associated with metabolic-related variables in postoperative patients with early-stage breast cancer. *Chin. J. Cancer Res.* 30:340–350, 2018.
- ⁵⁰Soukas, A., N. D. Succi, B. D. Saatkamp, S. Novelli, and J. M. Friedman. Distinct transcriptional profiles of adipogenesis in vivo and in vitro. *J. Biol. Chem.* 276:34167–34174, 2001.
- ⁵¹Tien, J., J. G. Truslow, and C. M. Nelson. Modulation of invasive phenotype by interstitial pressure-driven convection in aggregates of human breast cancer cells. *PLoS ONE* 7:e45191, 2012.
- ⁵²Tien, J., Y. W. Dance, U. Ghani, A. J. Seibel, and C. M. Nelson. Interstitial hypertension suppresses escape of human breast tumor cells via convection of interstitial fluid. *Cell. Mol. Bioeng.* 14:147–159, 2021.
- ⁵³Tiwari, P., A. Blank, C. Cui, K. Q. Schoenfelt, G. Zhou, Y. Xu, G. Khramtsova, F. Olopade, A. M. Shah, S. A. Khan,

- M. R. Rosner, and L. Becker. Metabolically activated adipose tissue macrophages link obesity to triple-negative breast cancer. *J. Exp. Med.* 216:1345–1358, 2019.
- ⁵⁴Verboven, K., K. Wouters, K. Gaens, D. Hansen, M. Bijnen, S. Wetzels, C. D. Stehouwer, G. H. Goossens, C. G. Schalkwijk, E. E. Blaak, and J. W. Jocken. Abdominal subcutaneous and visceral adipocyte size, lipolysis and inflammation relate to insulin resistance in male obese humans. *Sci. Rep.* 8:4677, 2018.
- ⁵⁵Visser, T. D., J. L. Oud, and G. J. Brakenhoff. Refractive index and axial distance measurements in 3-D microscopy. *Optik* 90:17–19, 1992.
- ⁵⁶Wang, Y. Y., C. Attané, D. Milhas, B. Dirat, S. Dauvillier, A. Guerard, J. Gilhodes, I. Lazar, N. Alet, V. Laurent, S. Le Gonidec, D. Biard, C. Hervé, F. Bost, G. S. Ren, F. Bono, G. Escourrou, M. Prentki, L. Nieto, P. Valet, and C. Muller. Mammary adipocytes stimulate breast cancer invasion through metabolic remodeling of tumor cells. *JCI Insight* 2:e87489, 2017.
- ⁵⁷Weisberg, S. P., D. McCann, M. Desai, M. Rosenbaum, R. L. Leibel, and A. W. Ferrante. Obesity is associated with macrophage accumulation in adipose tissue. *J. Clin. Investig.* 112:1796–1808, 2003.
- ⁵⁸Wueest, S., R. A. Rapold, J. M. Rytka, E. J. Schoenle, and D. Konrad. Basal lipolysis, not the degree of insulin resistance, differentiates large from small isolated adipocytes in high-fat fed mice. *Diabetologia* 52:541–546, 2009.
- ⁵⁹Yang, F., A. Carmona, K. Stojkova, E. I. Garcia Huitron, A. Goddi, A. Bhushan, R. N. Cohen, and E. M. Brey. A 3D human adipose tissue model within a microfluidic device. *Lab Chip* 21:435–446, 2021.

Publisher's Note Springer Nature remains neutral with regard to jurisdictional claims in published maps and institutional affiliations.

Springer Nature or its licensor (e.g. a society or other partner) holds exclusive rights to this article under a publishing agreement with the author(s) or other rightsholder(s); author self-archiving of the accepted manuscript version of this article is solely governed by the terms of such publishing agreement and applicable law.

Supplementary Table 1: Demographic and clinical data for the ASC donors in this study.

	Donor	Age	Sex	BMI	Ethnicity / Race
Lean	1	49	Female	20.4	White, non-Hispanic
	2	47	Female	23.5	White, non-Hispanic
	3	49	Female	24.7	White, non-Hispanic
	4	41	Female	24.9	White, non-Hispanic
Obese	5	49	Female	36.8	Black
	6	47	Female	36.8	White, non-Hispanic
	7	23	Female	38.6	White, non-Hispanic
	8	44	Female	41.8	White, non-Hispanic
	9	47	Female	41.9	White, non-Hispanic
Overweight	10	19	Female	27.5	White, Hispanic
	11	30	Female	28.0	White, Hispanic

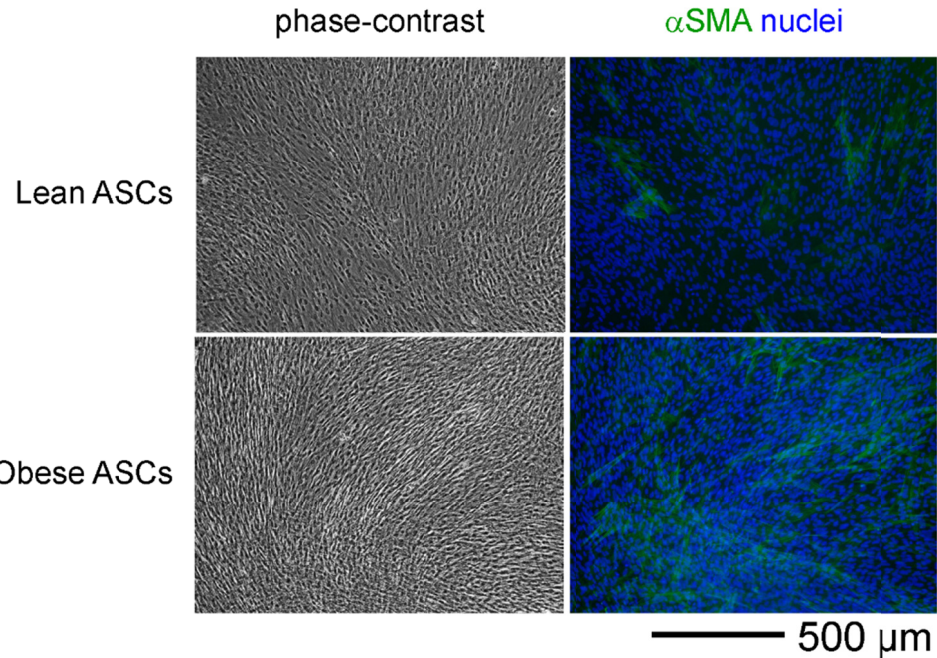
BMI, body mass index. All ASCs were derived from breast tissue.

Supplementary Figure 1: Phase-contrast (*left*) and immunofluorescence (*right*) images of lean and obese donor-derived ASCs stained for α SMA (*green*) and nuclei (*blue*) on coverslips.

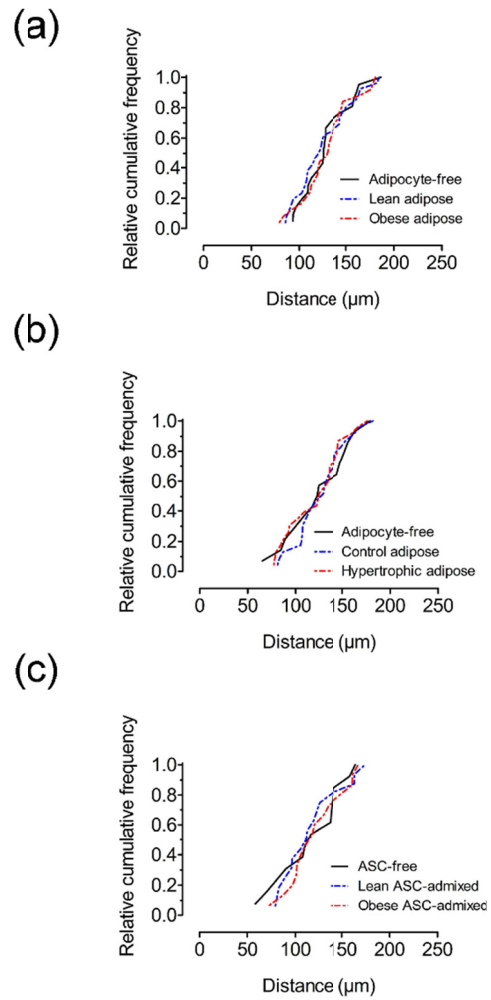
Supplementary Figure 2: Relative cumulative frequency distributions of initial (day 0) tumor-to-cavity distances. (a) For microtumors analyzed in Figure 3. (b) For microtumors analyzed in Figure 5. (c) For microtumors analyzed in Figure 6.

Supplementary Figure 3: Darcy permeability of cell-free collagen gels and adipose stroma. (a) Darcy permeability of adipocyte-free, lean adipose, and obese adipose stroma. (b) Darcy permeability of adipocyte-free, control adipose, and hypertrophic adipose stroma. Graphical bars indicate arithmetic means.

Supplementary Figure 1:



Supplementary Figure 2:



Supplementary Figure 3:

